Application of a silver–olefin coordination polymer as a catalytic curing agent for self-healing epoxy polymers

OPEN ACCESS
IOP Publishing
Smart Materials and Structures
Smart Mater. Struct. **24** (2015) 055004 (8pp)
doi:10.1088/0964-1726/24/5/055004

Application of a silver–olefin coordination polymer as a catalytic curing agent for self-healing epoxy polymers

D T Everitt[1], T S Coope[1], R S Trask[1], D F Wass[2] and I P Bond[1]

[1] ACCIS, Department of Aerospace Engineering, Queen's Building, University Walk, University of Bristol, BS8 1TR, UK
[2] School of Chemistry, Cantock's Close, University of Bristol, BS8 1TS, UK

E-mail: daniel.everitt@bristol.ac.uk

Received 31 October 2014, revised 15 January 2015
Accepted for publication 22 February 2015
Published 9 April 2015

Abstract

A silver–olefin based coordination polymer was prepared in a simple, one step process to act as an initiator to facilitate the ring-opening polymerization of epoxides. Thermal analysis found the complex to be capable of curing a range of commercially available epoxy resins used in the manufacture of conventional composite materials. Curing of the oligomeric diglycidyl ether bisphenol A resin, Epon 828, in combination with a non-toxic solvent, ethyl phenylacetate, was studied by differential scanning calorimetry. The mechanical characterization of the resultant cured polymers was conducted by single lap shear tests. Tapered double cantilever beam (TDCB) test specimens containing 2.5 pph of silver–olefin initiator, both with and without embedded microcapsules, were analyzed for their healing performance. Healing efficiency values were found to be strongly dependent on the applied healing temperature. A mean recovery of 74% fracture load was found in TDCB samples after being healed at 70 °C for 48 h.

Keywords: self-healing, microcapsules, epoxy resins

(Some figures may appear in colour only in the online journal)

1. Introduction

The development of self-healing capabilities for bulk polymer and fibre reinforced polymer (FRP) materials has attracted a great deal of research interest in recent years. Drawing inspiration from nature, synthetic self-healing materials aim to reduce the burden of inspection, repair and replacement of damaged high performance components. Microcapsules, vascular networks and intrinsic healing chemistries have emerged as the three primary approaches to realize self-healing materials. A recent review by Blaiszik *et al* provides an excellent summary of research into each technique [1].

Intrinsic self-healing materials rely on a range of different reversible chemistries to repair damage [2–8]. This approach does not require the delivery of external healing agents, and thus does not encounter the difficulty of integrating systems such as microcapsules or vascules into the material. Intrinsic systems, however, are limited to small damage volumes, may require an external stimulus and require the fracture surfaces to be in close contact.

Mechanophore chemistry represents a growing and potentially significant area of research for intrinsic multi-functional materials, including progress toward damage visualization [9–11], self-healing [12–15], stress-responsive materials and dynamic cross-linking [16].

Vascular networks seek to allow repeated healing events, after damage has occurred, by either delivering an on-demand supply of healing agent from a large external reservoir of healing agents or via purged microvascules containing a continuous supply of healing agent. Such systems seek to

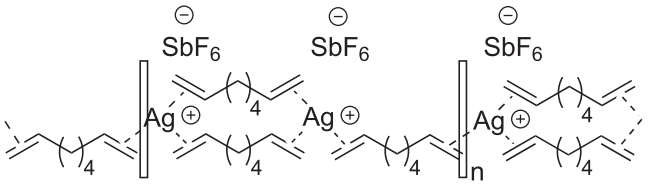

Figure 1. Structure of $\{[Ag(1, 7\text{-octadiene})_{1.5}]SbF_6\}_n$.

mimic vascular networks seen in the human body, and have also been shown to be capable of achieving high healing efficiencies [17–26].

The microcapsule approach involves dispersing encapsulated healing agents within a polymeric host material. Capsules rupture upon a damage event, infusing the damage site with healing agent and effecting repair. This technique has been researched extensively [15, 27–35], and is capable of achieving high healing efficiencies of >80%. Unfortunately, significant repeated healing diminishes rapidly with the consumption of capsules, and some voidage may occur after the healing process due to incomplete wet-out of the fracture plane. Furthermore, additional damage volume cannot be infused without either the addition of new material or the use of expanding healing agents.

Herein, we consider a novel catalytic curing agent for use in an epoxy-based self-healing material, investigated by exploiting microcapsules. The underlying chemistry presented in this paper is not limited to the microcapsule method and has also been shown to be applicable to vascular systems in other preliminary studies. Since the application of Grubbs' catalyst in self-healing polymers [27], a wide range of catalysts have been applied to the field of self-healing materials. While epoxy has most commonly been employed as the host matrix material, due to its high strength and low shrinkage, relatively few catalysts capable of polymerising epoxy monomers for self-healing have been investigated. Commonly used healing resins include poly(dicyclopentadienyl) [26–29] and polydimethylsiloxane [36, 37].

It is advantageous to ensure compatibility between the self-healing agent polymer and the host matrix material, in order to achieve good interfacial properties, and hence high healing efficiency values. Catalytic systems previously employed for epoxy-based self-healing materials include a copper bromide-imidazole latent hardener ($CuBr_2(2\text{-MeIm})_4$) [33–35], scandium(III) triflate ($Sc(OTf)_3$) [34], and aluminium(III) triflate ($Al(OTf)_3$) [32, 38].

In this paper is presented the silver–olefin coordination polymer $\{[Ag(1,7\text{-octadiene})_{1.5}]SbF_6\}_n$ (figure 1), first investigated for electron beam curing of epoxies by Barriau *et al* [39], and which herein shall be referred to as AgOlefin, as a viable catalyst for epoxy-based polymers self-healing agents. This catalyst is applied in conjunction with poly(urea-formaldehyde) microcapsules containing diglycidyl ether bisphenol A (DGEBA) epoxy monomer and ethyl phenylacetate (EPA) solvent, to produce a structural polymer capable of autonomous self-healing. The general mechanism of self-healing seen in systems of this type is depicted in figure 2.

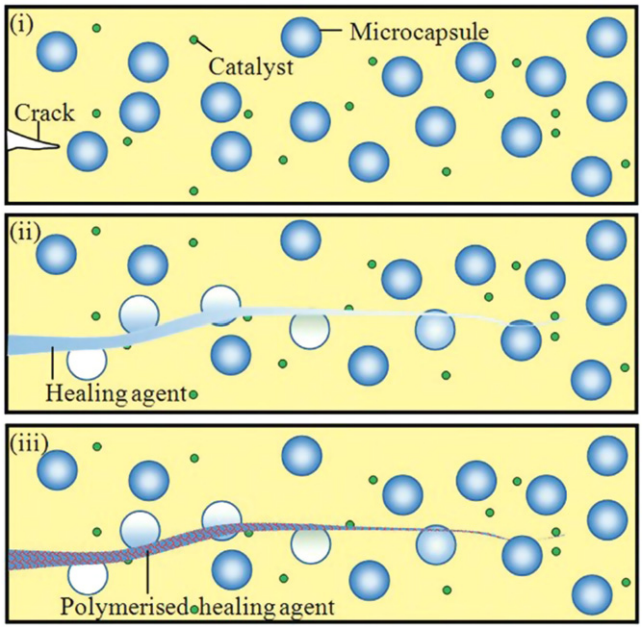

Figure 2. Healing mechanism in embedded catalyst/microencapsulated monomer healing systems. (i) Crack initiation. (ii) Crack propagation and microcapsule rupture, bringing monomer into contact with self-healing agent. (iii) Polymerization of the released monomer 'heals' the damage, allowing a recovery in mechanical performance. Reproduced with permission from T S Coope et al 2011 *Adv. Funct. Mater.* **21** 4624–31. Copyright © 2011 WILEY-VCH Verlag GmbH & Co. KGaA, Weinheim.

Differential scanning calorimetry (DSC) was used initially to conduct thermal cure analysis on a number of commercial epoxy resins, to demonstrate that the complex was capable of efficiently initiating ring-opening polymerization of epoxy resin in all cases. Single lap shear (SLS) testing was conducted to provide initial mechanical characterization of the healing resin, under a mixed-mode loading scenario. Finally, healing performance of the AgOlefin resin system was analyzed using a tapered double cantilever beam (TDCB) test specimen geometry [40, 41] cast from Epon 828 epoxy resin and diethylenetriamine (DETA) cross-linking agent. A premixed solution of Epon 828 epoxy and the non-toxic solvent diluent, EPA at 25 wt%, was used as the healing monomer. Delivery of the monomer was achieved by either manual injection to the fracture surface or by inclusion of microcapsules within the TDCB test specimens. The microcapsule system achieved a peak recovery of 74% in fracture load.

2. Results

2.1. Thermal cure analysis

The capacity of AgOlefin to cure four commercially available epoxy monomers was initially investigated using DSC, as part of a feasibility study to determine suitable candidate self-healing agents. The investigated epoxies were: *N*, *N*, *N*, *N*-tetraglycidyl-4, 4-diaminodiphenyl-methane, triglycidyl-*p*-

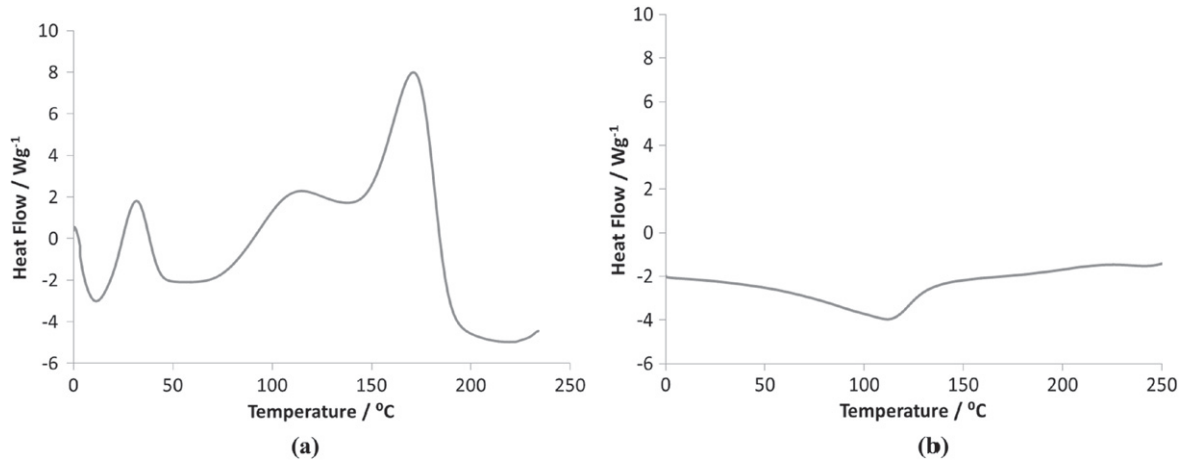

Figure 3. (a) 2.5 pph AgOlefin in Epon828/EPA (25 wt%) (b) Epon 828/EPA (25 wt%) with no catalytic initiator.

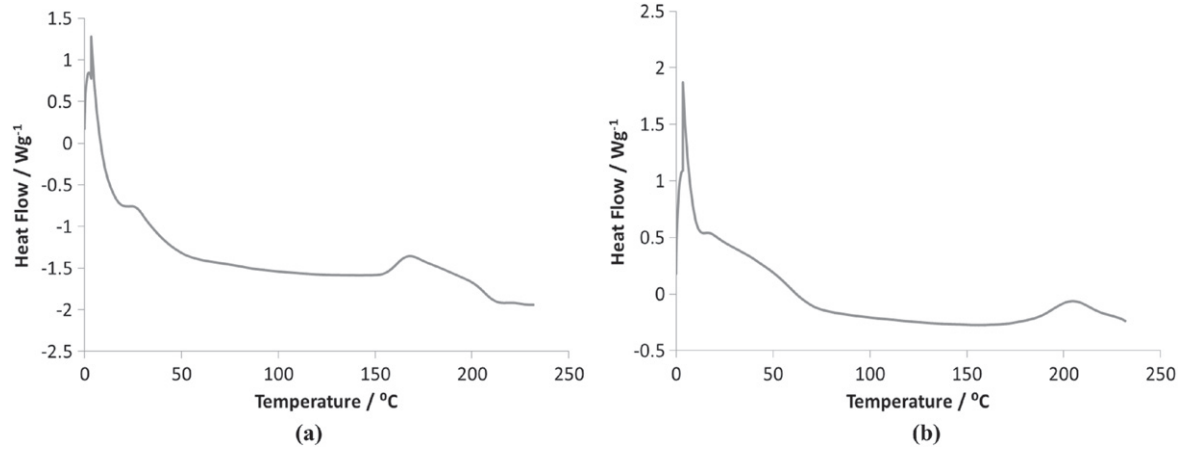

Figure 4. Modulated DSC analysis of 2.5 pph AgOlefin in Epon828/EPA (25 wt%) following (a) 48 h at 45 °C and (b) 48 h at 70 °C. In both cases no significant residual cure exotherm is detected.

aminophenol, (Poly[(phenyl glycidyl ether)-*co*-formaldehyde]) (DEN 431) and the oligomeric DGEBA (Epon 828). Curing of all resins by AgOlefin was confirmed by DSC analysis. Epon 828 was selected as the resin of choice for further study due to having lower viscosity than the alternatives and to allow for comparison to previous work of this nature [32].

A catalyst loading of 2.5 pph was added to the respective epoxy monomers and approximately 10 mg of solution was placed in a Tzero Aluminium Hermetic Pan. Samples were analyzed by modulated DSC (MDSC). Modulation amplitude = ±1 °C. Ramp rate = 10 °C min^{-1}. Nitrogen flow rate = 50 mL min^{-1}.

In order to ensure complete mixing of the initiator into the epoxy monomer, EPA was used as a diluent. Following solvation of the AgOlefin in EPA the solution was thoroughly mixed with the epoxy monomer prior to DSC analysis. MDSC analysis of 2.5 pph AgOlefin in Epon 828/EPA (25 wt%) can be seen in figure 3(a). DSC was also carried out on Epon 828/EPA (25 wt%) without any AgOlefin present in order to determine if any homopolymerization of the resin is taking place. Figure 3(b) shows no evidence of significant thermally induced homopolymerization. A small endothermic peak attributed to evaporation of the EPA can be seen at approximately 120 °C.

Three temperatures were selected for the healing study; 45 °C, 60 °C and 70 °C. 45 °C was selected as a starting temperature to enable comparison of results to previous work in the field [32], with higher temperatures subsequently investigated to determine the influence of temperature on healing efficiency. Temperatures above 70 °C were not investigated in this study as a longer term aim of this research is to implement the healing system within FRPs. Exposure to temperatures approaching those used during cure for long durations may lead to thermal ageing of FRPs and degradation of their performance. DSC analysis was carried out after exposure of the resin to healing conditions (48 h at the above temperatures) in order to determine the degree of cure. At both 45 °C and 70 °C near complete cure can be seen (figure 4). However, the higher glass transition temperature (table 1) resulting from curing at 70 °C indicates that the conversion process is not complete following 48 h at 45 °C. While no residual cure exotherm can be seen in figure 4(a), this only indicates that the resin is close to fully cured. In samples where no residual cure exotherm can be detected, T_g analysis can be used to trace the degree of cure relative to a

Table 1. Glass transition temperatures of 2.5 pph AgOlefin in Epon/EPA (25 wt%).

Cure temperature/°C	T_g/°C
45	43
70	53

benchmark sample [42], which in this case is obtained from curing the resin at 70 °C.

2.2. Healing resin analysis

SLS tests were conducted in accordance with ASTM D 5868 [43] in order to characterise the fundamental mechanical performance of the cured healing agents. Specimen failure loads and lap shear strengths are provided in table 2.

While the AgOlefin resin systems yield poor mechanical properties relative to a baseline Epon 828/DETA the results are typical for resins cured with low loadings of catalytic initiators.

2.3. Healing

All self-healing data was acquired using TDCB specimens as developed by Beres *et al* [40, 41] dimensions are given in figure 5.

All TDCBs were cast from Epon828 epoxy resin with 12 pph of DETA cross-linking agent. The degassed resin was cast in silicone moulds for a minimum of 7 days at ambient temperature.

The specimen geometry encourages crack propagation through the central trench region, thereby reducing the volume of functionalised material required to assess healing. The trenches were also cast from Epon 828/DETA. Manual healing specimens also contained 2.5 pph of dispersed AgOlefin catalyst. Microcapsule specimens contained 2.5 pph of dispersed AgOlefin catalyst together with 20 pph of DGEBA/EPA filled microcapsules, producing a material of the type depicted in figure 2.

All specimens were pre-cracked with a sharp razor blade to encourage crack propagation along the central trench region. A 3 mm diameter hole was drilled into the end of the trench to act as a crack-stopper, discouraging total failure of the specimens.

Testing was conducted according to the protocol developed by White *et al* [27, 28] on an Instron 3343 test machine equipped with a 1 kN calibrated load cell at a displacement rate of 0.3 mm per minute. Benchmark data for the average failure load of a pure Epon 828/DETA test specimen was obtained in previous work by Coope *et al* [32] five specimens were tested and average failure load and displacement values of 68 N and 0.58 mm respectively were obtained.

Healing efficiencies (ζ) were determined, as percentages, from pristine (P_{pristine}) and healed (P_{healed}) fracture load values according to equation (1):

$$\zeta = 100\left(\frac{P_{\text{healed}}}{P_{\text{pristine}}}\right). \quad (1)$$

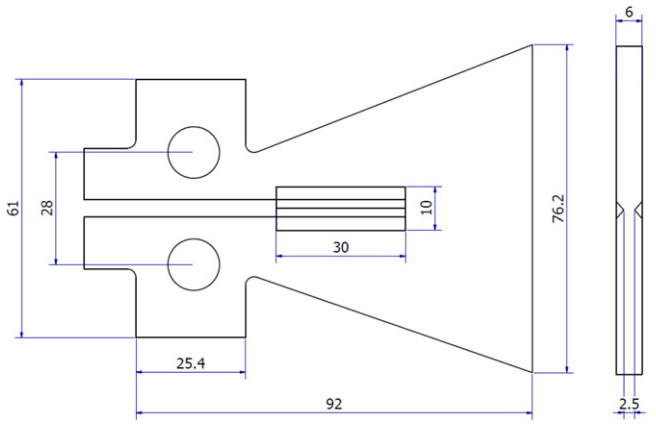

Figure 5. The tapered double cantilever beam (TDCB) geometry maintains constant fracture toughness at the crack tip, simplifying analysis. Dimensions are given in mm.

2.3.1. Manual. Manual delivery TDCBs were tested to obtain pristine performance prior to manual delivery of Epon 828 epoxy monomer to the fracture surface via a syringe. Excess monomer was removed and the specimens were sealed with one-sided adhesive release tape and healed for 48 h at 60 °C or 70 °C. Secondary testing was then carried out to allow determination of healing efficiency. This method has the advantage of providing good coverage and wet-out of injected monomer on the fracture surface.

An average failure load value of 66 N was found for pristine manual TDCB specimens.

Mean peak load recoveries of 51% and 65% were found in specimens healed at 60 °C and 70 °C, respectively. A representative load–displacement plot for a manual TDCB can be seen in figure 7(a).

2.3.2. Autonomous. Autonomous TDCBs were tested to obtain pristine performance. Monomer delivery was achieved in this case by the inclusion of microcapsules (2 pph) within the TDCB trenches (see section 2.3). Crack propagation causes exposure of embedded AgOlefin catalyst and rupture of the embedded microcapsules followed by the rapid infusion of the fracture surface with activated monomer (figures 2 and 6).

Healing was carried out at 45 °C, 60 °C and 70 °C prior to secondary testing. An average failure load of 100 N was found for pristine autonomous TDCB specimens. The increase in fracture toughness that was observed for autonomous test specimens, when compared to the manual specimens, was attributed to the presence of the embedded microcapsules. This was also shown to be consistent with previous observations made by Brown *et al* [44].

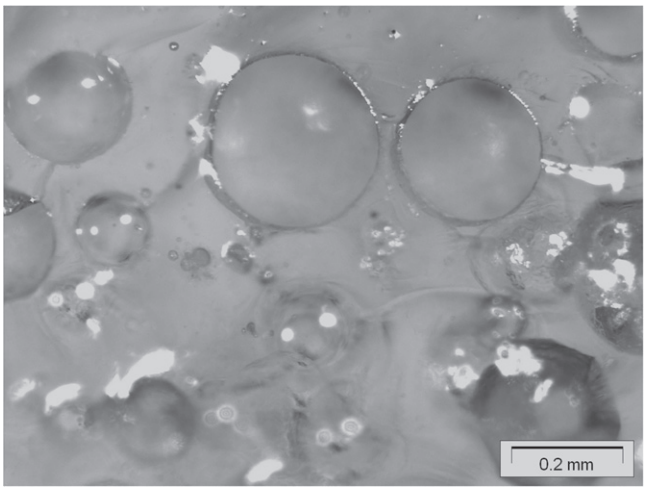

Figure 6. Optical micrograph showing burst microcapsules present on the fracture surface of an autonomous TDCB specimen.

Mean peak load recoveries of 24%, 59% and 74% were found in specimens healed at 45 °C, 60 °C and 70 °C respectively. A representative load–displacement plot for an autonomous TDCB can be seen in figure 7(b).

Healing results for both manual and autonomous TDCB specimens are summarized in figure 8. The expected trend of increased healing with increased temperature is clearly evident. Additionally, autonomous specimens, on average, achieved slightly higher healing efficiencies (+8.5%) than their manual counterparts. Manual injection results in a large amount of scatter, achieving healing efficiencies up to 36% lower and 20% higher than the autonomous average. This is thought to be due to inconsistencies in the healing agent delivery process.

3. Discussion

Two healing approaches, manual and autonomous, were investigated. Both methods were found to be capable of achieving high healing efficiencies. Initially manual injection was carried out to ascertain the viability of the AgOlefin catalyst in self-healing applications. In order to move to a more representative autonomous healing system, DGEBA/EPA microcapsules were embedded in the autonomous TDCB test specimens to remove the need for the manual injection of healing agent. Although only a relatively small volume of healing agent was delivered to the fracture surface, it was demonstrated that the inclusion of 20 pph of microcapsules was capable of resulting in high healing efficiencies. In addition, it showed that the presence of AgOlefin had no significant impact on the host polymer mechanical properties, whereas the presence of microcapsules does have a toughening effect, consistent with observations in the literature [44].

Microcapsules are capable of achieving slightly higher healing efficiencies than manual healing agent delivery, as well as exhibiting less scatter in the data. This is due to the fact that in autonomous specimens the delivery of healing agent to the fracture surface is localized and immediate. Inconsistent manual delivery is considered a source of increased variability of the results, as observed from test specimens.

As expected, increasing healing temperature resulted in improved healing efficiencies. While DSC analysis determined that healing at both 45 °C and 70 °C results in near complete cure of the epoxy (figure 3), it also indicates that higher temperatures result in a higher glass transition temperature (table 1). Additional thermal analysis could be carried out to determine the peak T_g obtainable from this system, however, the goal of this work is to achieve cure of the self-healing agent at ambient/modest temperatures, thus, the effect of high cure temperature/high T_g is of little practical interest in this study. Lap shear analysis also indicated that, as expected, cure temperature influences mechanical performance (table 2), and this is likely to be responsible for the variation in healing performance. Additionally, decreased viscosity of the healing agent at higher temperatures may allow for improved wet-out of the fracture surface. Improved healing is thought to be possible at further elevated temperatures, up to a critical point at which healing performance may plateau or decease. There is much scope for future work investigating the influence of a greater range of healing temperatures, although the goal is to achieve effective healing without resorting to high temperature processing.

The impact of varying catalyst loading on healing performance is not investigated in this study, but previous work with a different catalytic initiator ($Sc(OTf)_3$) has found it to be influential [38]. It is expected that through further optimization of the catalyst and microcapsule loading, along with healing temperature, higher healing efficiencies and much reduced healing times may be possible using the AgOlefin system. However, it is desirable to create a system which can provide effective healing under a wide range of conditions, rather than a highly a highly optimized system that provides excellent healing under very stringent conditions.

Specimens healed at all temperatures consistently fail in a more ductile manner than in the pristine tests. This observation is consistent with other TDCB healing studies [28, 32, 45], but is not observed in all cases [27, 46]. In this case the increased ductility is attributed to the mechanical properties of the healing polymer. While good adhesion between the fracture surfaces allows effective recovery of strength and stiffness, the ductile nature of the healing resin leads to less brittle failure of healed specimens compared to pristine.

4. Conclusions

It has been demonstrated that TDCB test specimens loaded with AgOlefin catalyst and DGEBA/EPA microcapsules are capable of undergoing healing after a 48 h heating period. The presence of the catalyst was seen to have no effect on the innate mechanical properties of the host matrix, while the presence of microcapsules resulted in some toughening, increasing peak load by 31%.

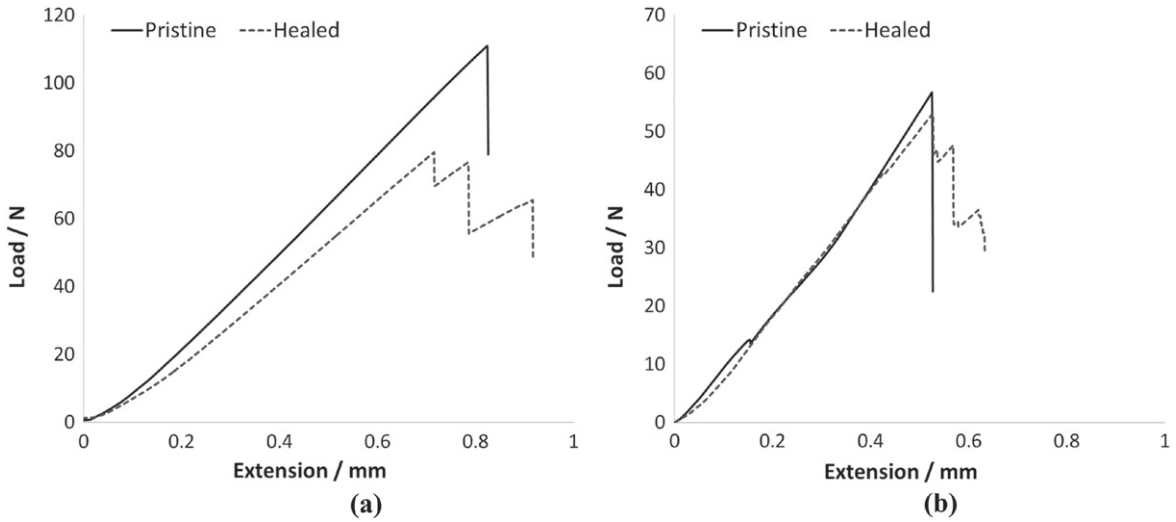

Figure 7. (a) Representative load–displacement plot for an autonomous TDCB healed at 60 °C. Specimen contained 2.5 pph dispersed AgOlefin catalyst and 20 pph DGEBA/EPA microcapsules, a 73.4% recovery in failure load can be seen. (b) Representative load–displacement plot for a manual TDCB healed at 70 °C. Specimen contained 2.5 pph dispersed AgOlefin catalyst, a 94.4% recovery in failure load can be seen.

Table 2. Lap shear strengths of specimens adhered with Epon/EPA (25 wt%), cured for 48 h at various temperatures.

Hardener	Cure temperature/°C	Failure load/N		Lap shear strength/MPa	
DETA (12 pph)	RT	8540	±719	13	±1
AgOlefin (2.5 pph)	45	70	±13	0.11	±0.02
AgOlefin (2.5 pph)	70	193	±96	0.30	±0.14

Manual injection of healing resin onto the fracture surface resulted in successful healing at both 60 °C and 70 °C. Autonomous specimens, containing both embedded AgOlefin catalyst and Epon 828/EPA microcapsules, were healed at 45 °C, 60 °C and 70 °C, and were shown to achieve 16% higher healing efficiencies on average than their manual injection counterparts. Autonomous specimens healed at 70 °C achieved an average healing efficiency of 74%.

Higher healing efficiencies seen at elevated temperatures are a direct effect of improved mechanical properties of the cured healing agent, as demonstrated by DSC and SLS testing. In addition, this is also attributed to improved wet-out of the fracture surfaces, as a result of a reduction in resin viscosity.

The potential for tuning silver coordination polymer-based self-healing catalysts will be investigated in future work, with a focus on temperature-stable silver–phosphine based healing agents. The potential for integrating these catalysts into FRP composite materials will also be investigated, with the aim of developing self-healing systems which are compatible with existing manufacturing processes.

5. Experimental

5.1. Synthesis of {[Ag(1, 7-octadiene)$_{1.5}$]SbF$_6$}$_n$

To a solution of $AgSbF_6$ (2 g, 5.83 mmol) in toluene (15 ml), was added 1, 7-octadiene (2 ml, 1.5 g, 13.5 mmol) dropwise in a nitrogen atmosphere. Solution was stirred overnight, yielding an off-white solid. Product was isolated by filtration and washed with toluene and pentane prior to drying in vacuo. Product was stored in air in an opaque vial. Elemental analysis calculated (%): C, 28.32; H, 4.16. Found: C, 27.12; H, 3.93. ^{1}H NMR (300 MHz, acetone-d^6): δ 1.36–1.47 (m, 4 H), 2.04-2.11 (m, 5 H), 2.99 (d, 1 H), 4.94–5.05 (m, 4 H), 5.82-5.96 (m, 2 H). ^{13}C NMR (75 MHz, acetone-d^6): δ 29.04 (septet), 205.4 (s). FTIR (nujol) (cm^{-1}) 3630, 3547, 2928, 2859, 1593, 1459, 1378, 1037, 964, 728, 663.

5.2. Microencapsulation methodology

Poly(urea-formaldehyde) microcapsules containing a solution of DGEBA and EPA (25 wt%) were synthesized according to methods pioneered by Brown *et al* [47] and adapted by Blaiszik *et al* [48].

A 30 mL solution of 2.5% (wt/vol) ethylene-maleic anhydride copolymer, urea (2.5 g), resorcinol (0.25 g) and ammonium chloride (0.25 g) was stirred for 10 min, prior to addition of a DGEBA/EPA (0.25 wt%) solution. NaOH solution was added to maintain a pH of 2.7–3.5. The solution was then stirred at 650 rpm for 10 min. Formalin (6.33 g) was then added and the temperature raised to 55 °C. These conditions were maintained for 4 h. The resulting microcapsules were then cooled for 6 h before filtration and air-drying.

Microcapsules were found by microscopy to have mean diameters of 103 ± 38 μm. (The number of samples was 150.)

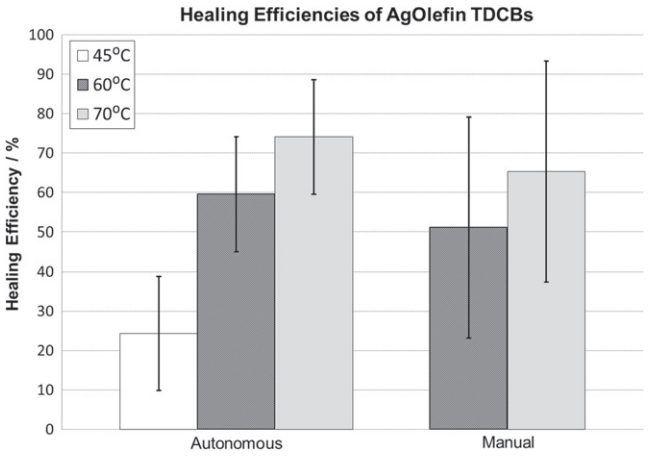

Figure 8. Summary of healing results. Error bars represent the standard deviation. Healing was carried out at 45 °C, 60 °C and 70 °C. Mean healing efficiencies are calculated from a minimum of five specimens.

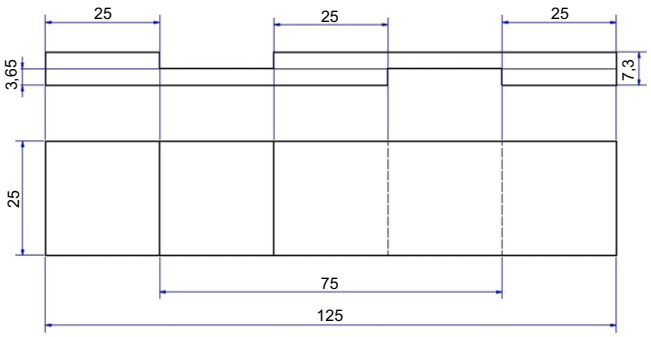

Figure 9. Lap shear specimen dimensions.

5.3. Differential scanning calorimetry

All DSC analysis was carried out on a TA Instruments Q2000 DSC using TA Instruments Tzero Aluminium Hermetic Pans.

MDSC runs were carried out with a ramp rate of 10 °C min^{-1} and modulation amplitude of 1 °C every 60 s.

5.4. SLS specimens

Lap shear specimens were manufactured from Gurit SE70 carbon fibre/epoxy prepreg according to ASTM D 5868. Dimensions can be found in figure 9. Following the application of epoxy resin to both bond surfaces, the specimens were clamped together and cured. The resulting bond-line thickness was found by microscopy to be 50 μm.

5.5. TDCB specimens/healing analysis

All TDCBs were cast from 100 parts Epon 828 resin with 12 pph DETA cross-linking agent. The degassed resin was cast in silicone moulds for a minimum of 7 days at ambient temperature.

TDCB trenches were also cast from Epon 828/DETA. Manual healing specimens contained 2.5 pph of AgOlefin catalyst. Microcapsule specimens contained 2.5 pph of AgOlefin catalyst along with 20 pph of DGEBA/EPA microcapsules.

All specimens were pre-cracked with a razor blade to encourage crack propagation along the trench. A 3 mm diameter hole was drilled into the end of the trench to act as a crack-stopper, discouraging total failure of the specimens.

Testing was conducted on an Instron 3343 test machine with a calibrated 1 kN load call at a rate of 0.3 mm min^{-1}.

Acknowledgments

We would like to thank the UK Engineering and Physical Sciences Research Council (EPSRC) [EP/G036772/1] for funding this research.

References

[1] Blaiszik B J, Kramer S L B, Olugebefola S C, Moore J S, Sottos N R and White S R 2010 Self-healing polymers and composites *Annu. Rev. Mater. Res.* **40** 179–211
[2] Chen X, Wudl F, Mal A K, Shen H and Nutt S R 2003 New thermally remendable highly cross-linked polymeric materials *Macromolecules* **36** 1802–7
[3] Varley R J and van der Zwaag S 2008 Towards an understanding of thermally activated self-healing of an ionomer system during ballistic penetration *Acta Mater.* **56** 5737–50
[4] Luo X, Ou R, Eberly D E, Singhal A, Viratyaporn W and Mather P T 2009 A thermoplastic/thermoset blend exhibiting thermal mending and reversible adhesion *ACS Appl. Mater. Interfaces* **1** 612–20
[5] Cordier P, Tournilhac F, Soulié-Ziakovic C and Leibler L 2008 Self-healing and thermoreversible rubber from supramolecular assembly *Nature* **451** 977–80
[6] McGarel O and Wool R 1987 Craze growth and healing in polystyrene *J. Polym. Sci.* B **25** 2541–60
[7] O'Connor K M and Wool R P 1980 Optical studies of void formation and healing in styrene-isoprene-styrene block copolymers *J. Appl. Phys.* **51** 5075
[8] Yang T, Wang C H, Zhang J, He S and Mouritz A P 2012 Toughening and self-healing of epoxy matrix laminates using mendable polymer stitching *Compos. Sci. Technol.* **72** 1396–401
[9] Potisek S L, Davis D A, Sottos N R, White S R and Moore J S 2007 Mechanophore-linked addition polymers *J. Am. Chem. Soc.* **129** 13808–9
[10] Davis D A *et al* 2009 Force-induced activation of covalent bonds in mechanoresponsive polymeric materials *Nature* **459** 68–72
[11] Cho S-Y, Kim J-G and Chung C-M 2008 A fluorescent crack sensor based on cyclobutane-containing cross-linked polymers of tricinnamates *Sensors Actuators* B **134** 822–5
[12] Black A L, Orlicki J A and Craig S L 2011 Mechanochemically triggered bond formation in solid-state polymers *J. Mater. Chem.* **21** 8460
[13] Paulusse J M J and Sijbesma R P 2008 Selectivity of mechanochemical chain scission in mixed palladium(II) and platinum(II) coordination polymers *Chem. Commun.* 4416–8
[14] Piermattei A, Karthikeyan S and Sijbesma R P 2009 Activating catalysts with mechanical force *Nat. Chem.* **1** 133–7
[15] Jakobs R T M and Sijbesma R P 2012 Mechanical activation of a latent olefin metathesis catalyst and persistence of its active species in romp *Organometallics* **31** 2476–81

[16] Black A L, Lenhardt J M and Craig S L 2011 From molecular mechanochemistry to stress-responsive materials *J. Mater. Chem.* **21** 1655
[17] Bleay S M, Loader C B, Hawyes V J, Humberstone L and Curtis P T 2001 A smart repair system for polymer matrix composites *Composites* A **32** 1767–76
[18] Pang J W C and Bond I P 2005 'Bleeding composites'—damage detection and self-repair using a biomimetic approach *Composites* A **36** 183–8
[19] Pang J W C and Bond I P 2005 A hollow fibre reinforced polymer composite encompassing self-healing and enhanced damage visibility *Compos. Sci. Technol.* **65** 1791–9
[20] Williams G, Trask R S and Bond I P 2007 A self-healing carbon fibre reinforced polymer for aerospace applications *Composites* A **38** 1525–32
[21] Trask R S and Bond I P 2006 Biomimetic self-healing of advanced composite structures using hollow glass fibres *Smart Mater. Struct.* **15** 704–10
[22] Trask R S, Williams G J and Bond I P 2007 Bioinspired self-healing of advanced composite structures using hollow glass fibres *J. R. Soc. Interface/R. Soc.* **4** 363–71
[23] Williams H R, Trask R S, Weaver P M and Bond I P 2008 Minimum mass vascular networks in multifunctional materials *J. R. Soc. Interface* **5** 55–65
[24] Norris C J, Bond I P and Trask R S 2013 Healing of low-velocity impact damage in vascularised composites *Composites* A **44** 78–85
[25] Norris C J, Bond I P and Trask R S 2011 Interactions between propagating cracks and bioinspired self-healing vascules embedded in glass fibre reinforced composites *Compos. Sci. Technol.* **71** 847–53
[26] Toohey K S, Sottos N R, Lewis J a, Moore J S and White S R 2007 Self-healing materials with microvascular networks *Nat. Mater.* **6** 581–5
[27] White S R, Sottos N R, Geubelle P H, Moore J S, Kessler M R, Sriram S R, Brown E N and Viswanathan S 2001 Autonomic healing of polymer composites *Nature* **409** 794–7
[28] Brown E, Sottos N R and White S R 2002 Fracture testing of a self-healing polymer composite *Exp. Mech.* **42** 372–9
[29] Kamphaus J and Rule J 2008 A new self-healing epoxy with tungsten (VI) chloride catalyst *J. R. Soc. Interface* **5** 95–103
[30] Wilson G O, Porter K A, Weissman H, White S R, Sottos N R and Moore J S 2009 Stability of second generation grubbs' alkylidenes to primary amines: formation of novel ruthenium-amine complexes *Adv. Synth. Catalysis* **351** 1817–25
[31] Wilson G O, Caruso M M, Reimer N T, White S R, Sottos N R and Moore J S 2008 Evaluation of ruthenium catalysts for ring-opening metathesis polymerization-based self-healing applications *Chem. Mater.* **20** 3288–97
[32] Coope T S, Mayer U F J, Wass D F, Trask R S and Bond I P 2011 Self-healing of an epoxy resin using scandium(III) triflate as a catalytic curing agent *Adv. Funct. Mater.* **21** 4624–31
[33] Yin T, Rong M, Zhang M and Yang G 2007 Self-healing epoxy composites—preparation and effect of the healant consisting of microencapsulated epoxy and latent curing agent *Compos. Sci. Technol.* **67** 201–12
[34] Yin T, Zhou L, Rong M Z and Zhang M Q 2008 Self-healing woven glass fabric/epoxy composites with the healant consisting of micro-encapsulated epoxy and latent curing agent *Smart Mater. Struct.* **17** 015019
[35] Yin T, Rong M Z, Zhang M Q and Zhao J Q 2009 Durability of self-healing woven glass fabric/epoxy composites *Smart Mater. Struct.* **18** 074001
[36] Keller M W, White S R and Sottos N R 2007 A self-healing poly(dimethyl siloxane) elastomer *Adv. Funct. Mater.* **17** 2399–404
[37] Mangun C L, Mader A C, Sottos N R and White S R 2010 Self-healing of a high temperature cured epoxy using poly (dimethylsiloxane) chemistry *Polymer* **51** 4063–8
[38] Coope T S, Wass D F, Trask R S and Bond I P 2013 Metal triflates as catalytic curing agents in self-healing fibre reinforced polymer composite materials *Macromol. Mater. Eng.* **299** 208–18
[39] Barriau E, Schmidt-freytag U, Roth M, Gehring J, Simon N, Wolff-fabris F, Altstaedt V, Do M, Arnold U and Du D 2008 Silver olefin complexes : highly efficient initiators for the electron beam curing of epoxy resins *Macromolecules* **41** 3779–81
[40] Beres W, Koul A and Thamburaj R 1997 A tapered double-cantilever-beam specimen designed for constant-k testing at elevated temperatures *J. Test. Eval.* **25** 536–42
[41] Rule J D, Sottos N R and White S R 2007 Effect of microcapsule size on the performance of self-healing polymers *Polymer* **48** 3520–9
[42] Scheirs J 2000 *Compositional and Failure Analysis of Polymers: A Practical Approach* (New York: Wiley)
[43] ASTM International 2003 ASTM Standard D 5868 2001 *Lap Shear Adhesion for Fiber Reinforced Plastic (FRP)* (West Conshohocken, PA: ASTM International) doi:10.1520/D5868 (www.astm.org)
[44] Brown E N, White S R and Sottos N R 2004 Microcapsule induced toughening in a self-healing polymer composite *J. Mater. Sci.* **39** 1703–10
[45] Meure S, Wu D Y and Furman S 2009 Polyethylene-co-methacrylic acid healing agents for mendable epoxy resins *Acta Mater.* **57** 4312–20
[46] Jin H, Mangun C L, Stradley D S, Moore J S, Sottos N R and White S R 2012 Self-healing thermoset using encapsulated epoxy-amine healing chemistry *Polymer* **53** 581–7
[47] Brown E N, Kessler M R, Sottos N R and White S R 2003 *In situ* poly(urea-formaldehyde) microencapsulation of dicyclopentadiene *J. Microencapsulation* **20** 719–30
[48] Blaiszik B J, Caruso M M, McIlroy D a., Moore J S, White S R and Sottos N R 2009 Microcapsules filled with reactive solutions for self-healing materials *Polymer* **50** 990–7